Supporting information

Boron Doping in Carbon Layer: A Facile Strategy to Boost Electrochemical Performance of $Na_2FeTi(PO_4)_3$@C

Ziyan Wang†, Zhilong Tan†, Yuening Zou, Rongzheng Zhang, Peng Zhou, Diye Wei, Zhifeng Huang, Hai Hu, Li Liu**

National Local Joint Engineering Laboratory for Key Materials of New Energy Storage Battery, Hunan Province Key Laboratory of Electrochemical Energy Storage and Conversion, Key Laboratory of Environmentally Friend Chemistry and Applications of Ministry of Education, School of Chemistry, Xiangtan University, Xiangtan 411105, China

† Corresponding author: These authors contributed equally to this work.
**Corresponding author at: School of Chemistry, Xiangtan University, Xiangtan 411105, China. E-mail addresses: huhai29@126.com (H. Hu), liulili1203@126.com (L. Liu).*

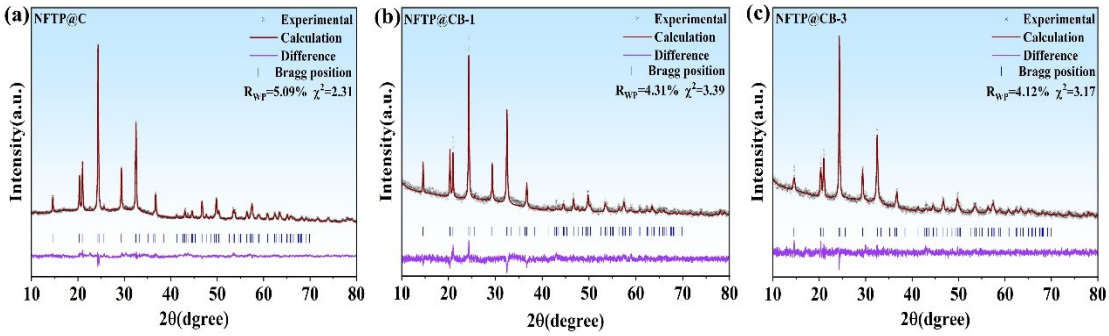

Figure S1. (a) Rietveld refinement of the XRD pattern for NFTP@C; (b) Rietveld refinement of the XRD pattern for NFTP@CB-1; (c) Rietveld refinement of the XRD pattern for NFTP@CB-3.

Table S1. Lattice parameters of NFTP@CB-x (x = 0,1,2,3).

	NFTP@C	**NFTP@CB-1**	**NFTP@CB-2**	**NFTP@CB-3**
a=b (Å)	8.47871	8.48223	8.48925	8.49228
C (Å)	21.78385	21.79746	21.81578	21.82556
V ($Å^3$)	1356.204	1358.178	1361.551	1363.152

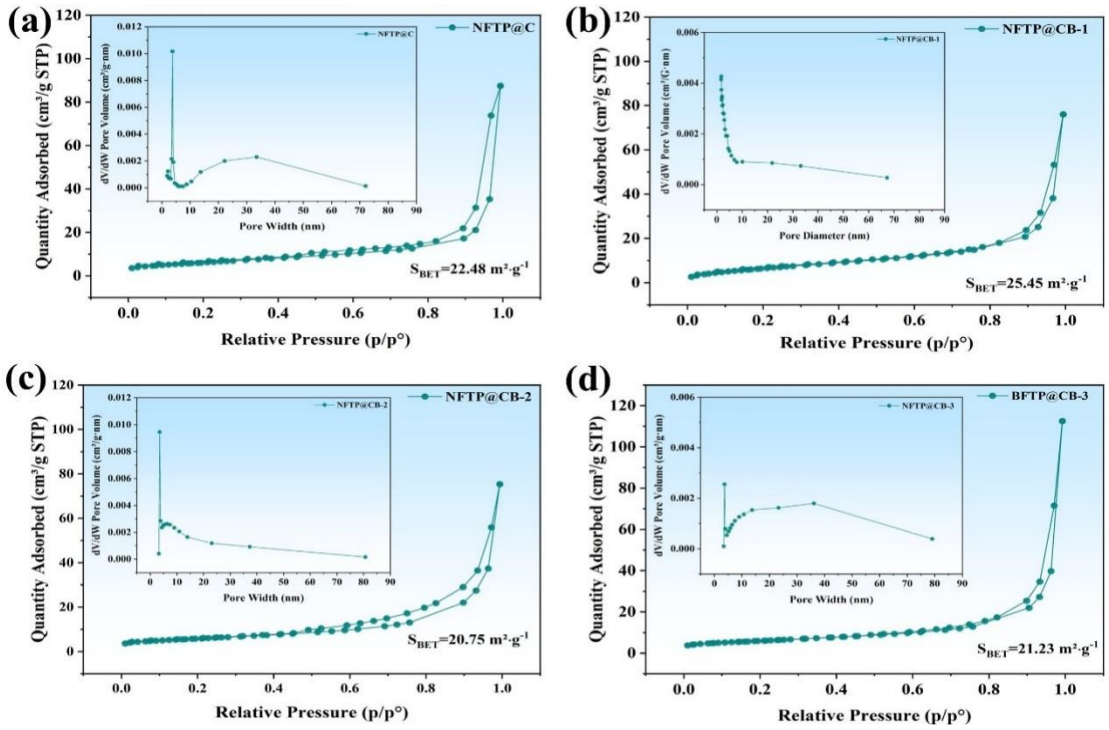

Figure S2. (a–d) N_2 adsorption–desorption isotherms and pore size distribution plots of NFTP@CB-x (x = 0,1,2,3) materials.

Table S2. (a–d) N_2 adsorption–desorption isotherms and pore size distribution plots of NFTP@CB-x (x = 0,1,2,3) materials.

Samples	**BET surface area (m^2 g^{-1})**	**Pore volume (cm^3 g^{-1})**	**Pore diameter (nm)**
NFTP@C	22.478	0.135	24.072
NFTP@CB-1	25.447	0.118	18.489
NFTP@CB-2	20.752	0.117	22.465
NFTP@CB-3	21.232	0.174	32.79

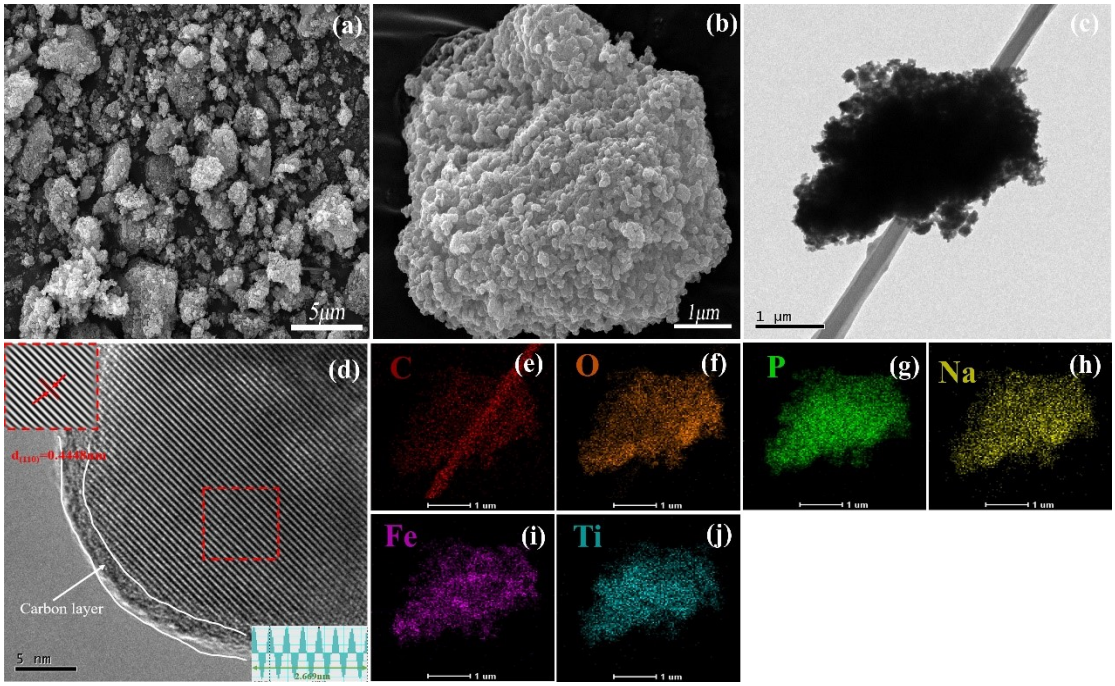

Figure S3. (a-c) SEM and TEM images of NFTP@C; (d) HRTEM image of NFTP@C; (e-j) EDS elemental mapping images of NFTP@C.

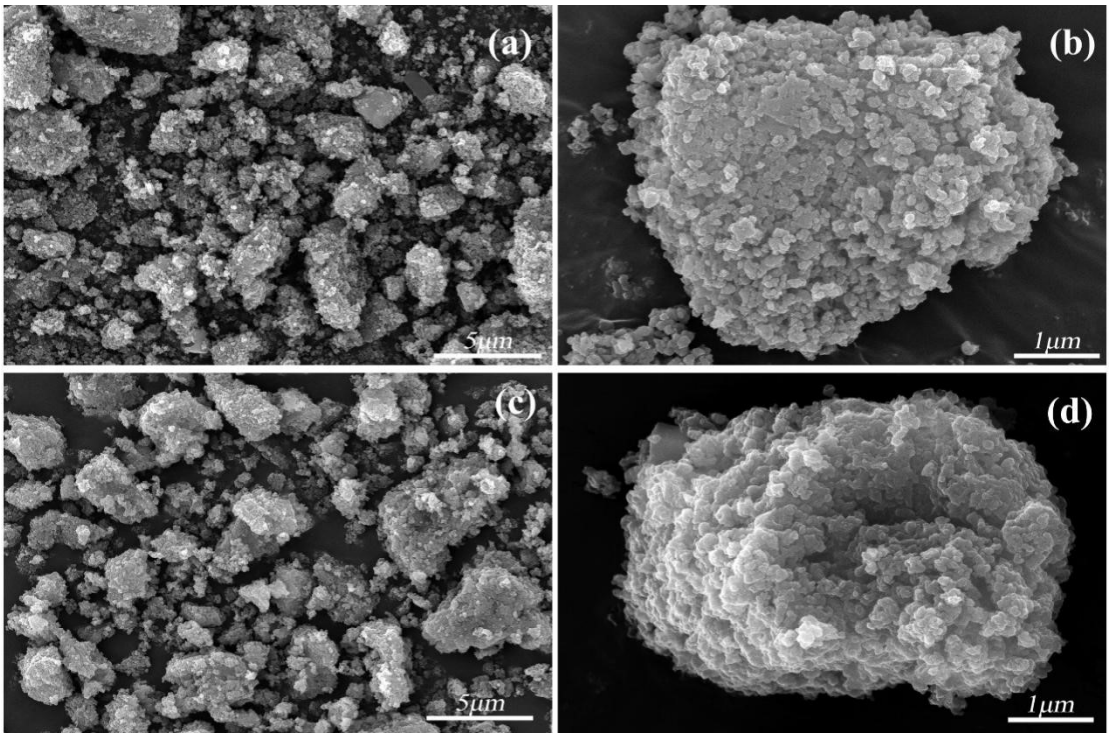

Figure S4. (a-b) SEM images of NFTP@CB-1; (c-d) SEM images of NFTP@CB-3.

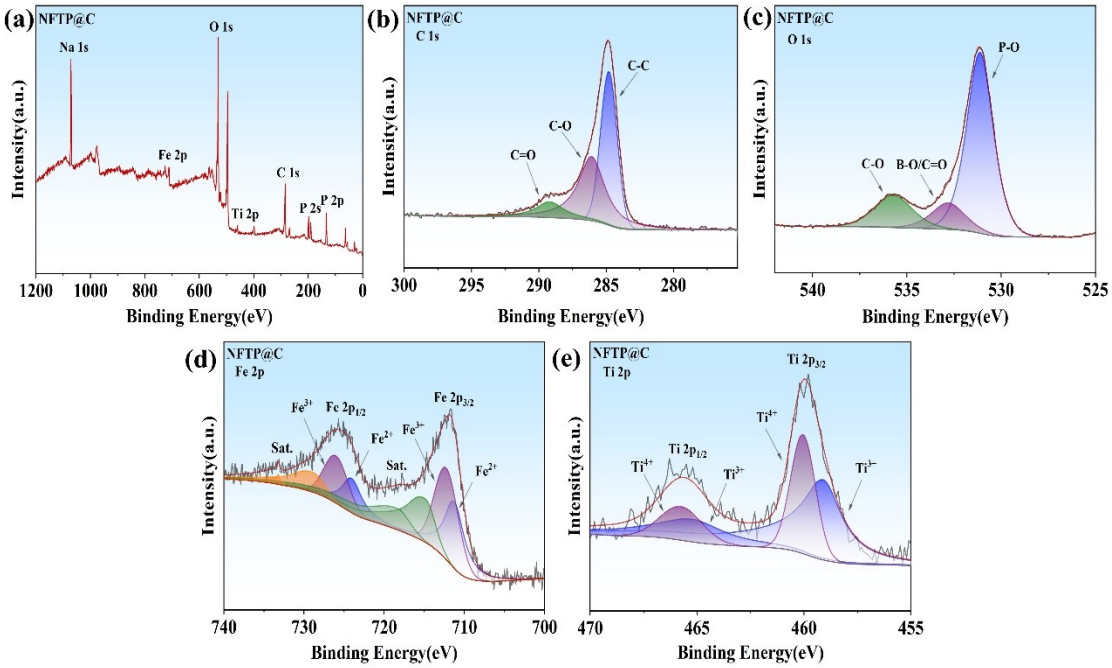

Figure S5. XPS spectra of NFTP@C: (a) survey spectrum; (b) high-resolution C 1s spectrum; (c) high-resolution O 1s spectrum; (d) high-resolution Fe 2p spectrum; (e) high-resolution Ti 2p spectrum.

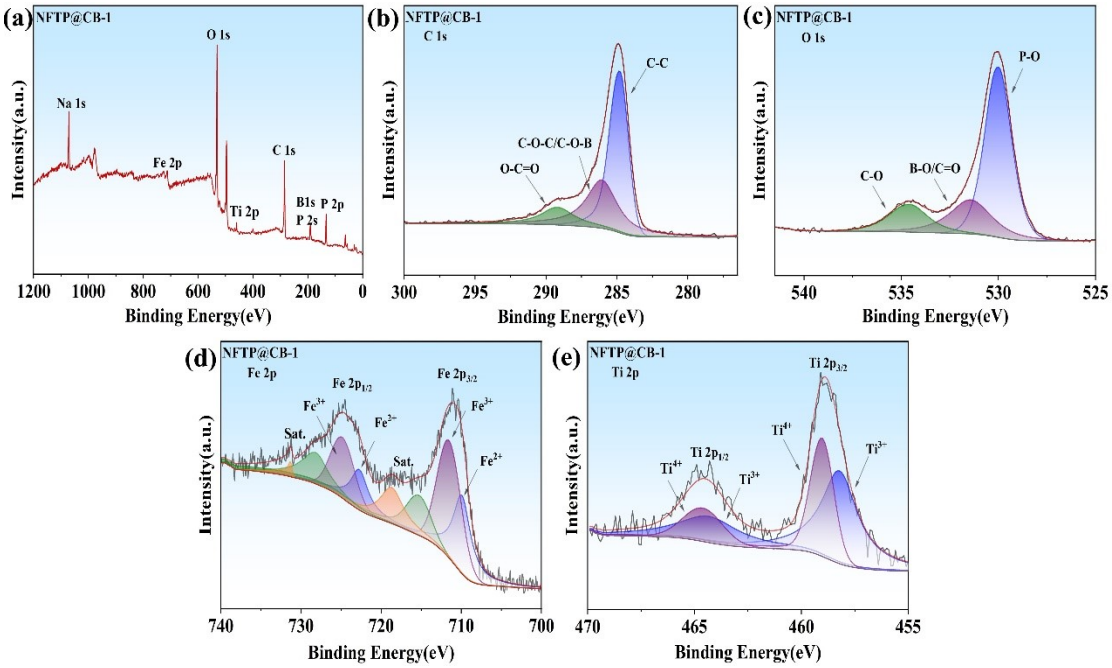

Figure S6. XPS spectra of NFTP@CB-1: (a) survey spectrum; (b) high-resolution C 1s spectrum; (c) high-resolution O 1s spectrum; (d) high-resolution Fe 2p spectrum; (e) high-resolution Ti 2p spectrum.

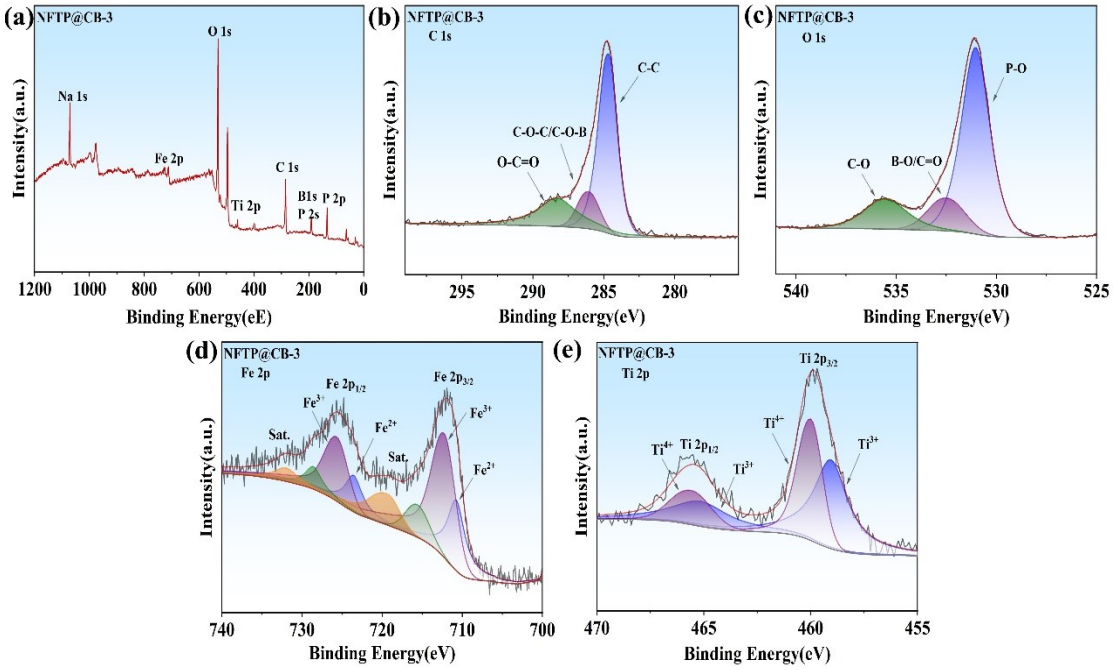

Figure S7. XPS spectra of NFTP@CB-3: (a) survey spectrum; (b) high-resolution C 1s spectrum; (c) high-resolution O 1s spectrum; (d) high-resolution Fe 2p spectrum; (e) high-resolution Ti 2p spectrum.

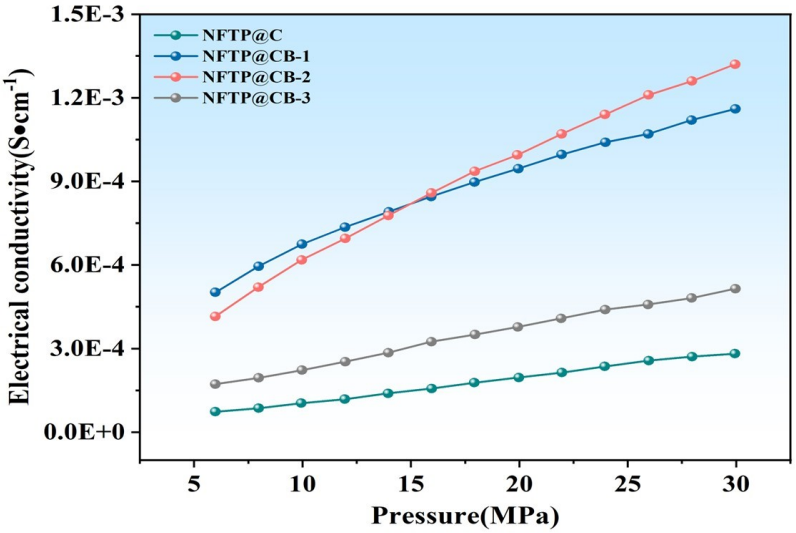

Figure S8. NFTP@CB-x (x=0,1,2,3) Four-probe measurement technique.

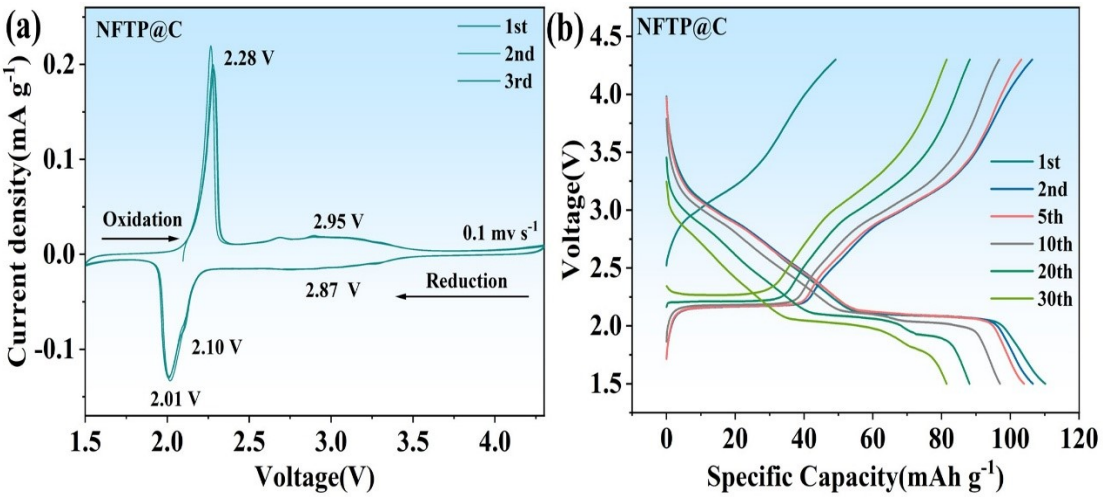

Figure S9. (a) CV curves of NFTP@C at a scan rate of 0.1 mV s^{-1} ; (b) GCD (galvanostatic charge – discharge) curves of NFTP@C at various current densities.

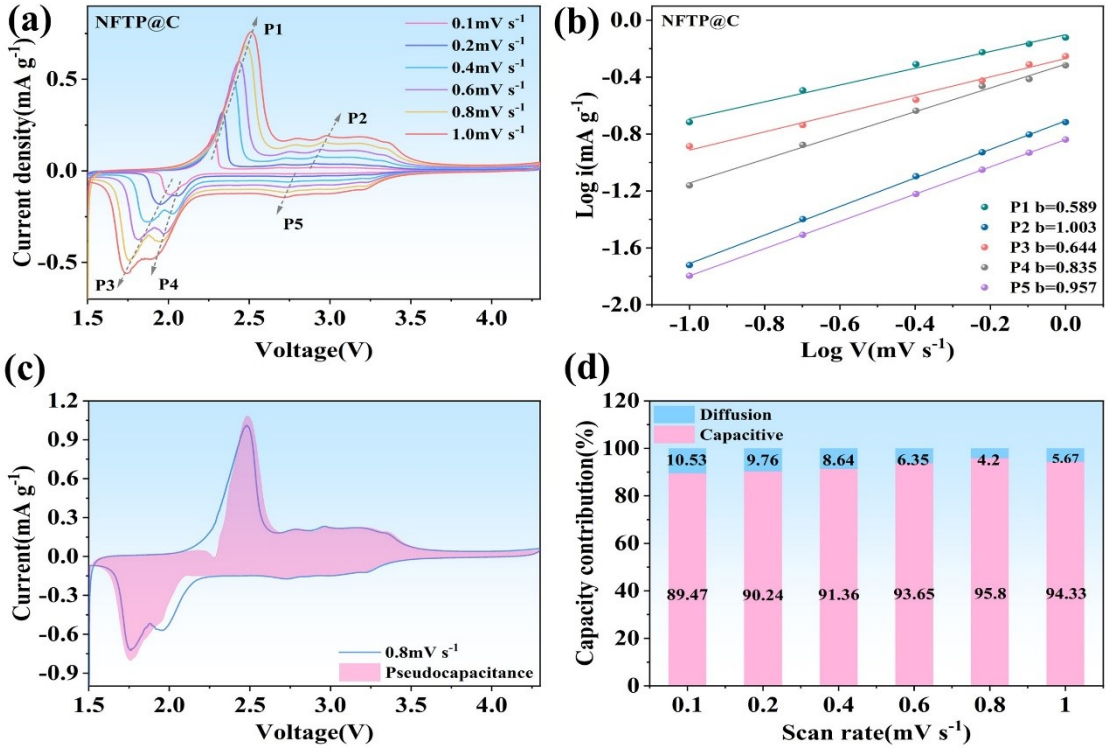

Figure S10. NFTP@C: (a) CV curves at various scan rates; (b) Linear relationship between log i and log v at different scan rates; (c) Pseudocapacitive contribution at

0.8 mV s^{-1} ; (d) Pseudocapacitive contribution ratios at different scan rates.

Table S3. The Rct and Rs values, as well as the Na^+ diffusion coefficients, of NFTP@CB-x (x = 0,1,2,3).

Samples	Rct (Ω)	Rs	D_{Na^+} (cm^2 S^{-1})
NFTP@C	269.5	12.49	2.54×10^{-17}
NFTP@CB-1	251.5	19.05	3.26×10^{-17}
NFTP@CB-2	207.5	9.24	8.30×10^{-17}
NFTP@CB-3	224.3	11.3	7.31×10^{-17}

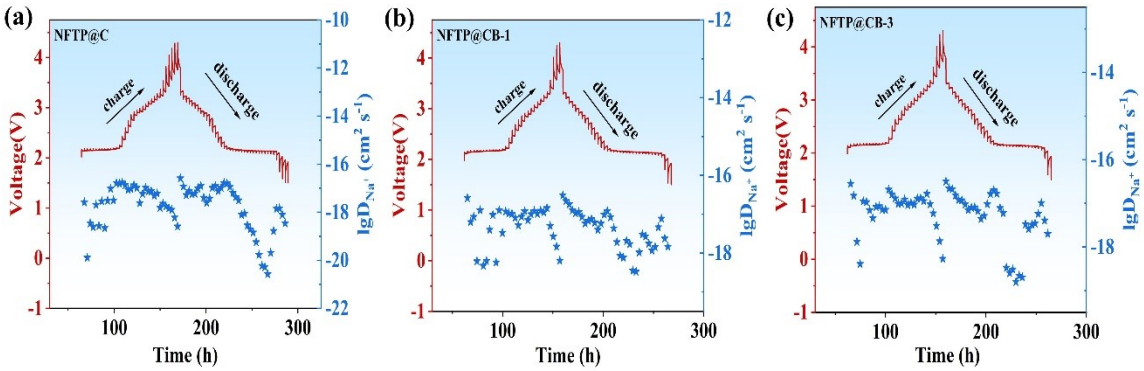

Figure S 11. NFTP@CB-x (x = 0,1,3): (a-c) GITT curves and the corresponding calculated log DNa^+ values.

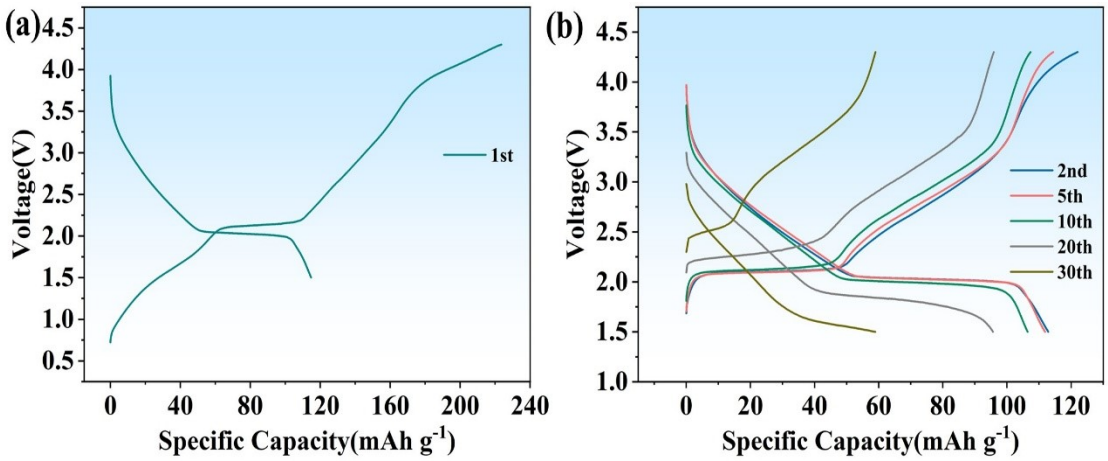

Figure S12. Galvanostatic charge–discharge (GCD) profiles of the NFTP@CB-2//HC full cell at various current densities: first cycle (a), and cycles 2, 5, 10, 20, and 30 (b).